Full Paper Transactions, SMiRT 28
Toronto, Canada, August 10-15, 2025
Division I

Fatigue Modelling of a Metastable Austenitic Stainless Steel Used in Nuclear Powerplant Components by Crystal Plasticity Finite Element Method

Christian Häffner[1], Sebastian Münstermann[2]

[1] PhD Candidate, Institute of Metal Forming at RWTH Aachen University, Germany (christian.haeffner@ibf.rwth-aachen.de)
[2]Professor, Institute of Metal Forming at RWTH Aachen University, Germany (sebastian.muenstermann@ibf.rwth-aachen.de)

ABSTRACT

Pipelines in nuclear power plants are often made of austenitic stainless steels. This material class includes, for example, the steel grade AISI 347, which is characterized by a metastable austenitic microstructure. Due to the cyclic loads occurring during operation, the metastable austenitic phase transforms into a martensitic phase through the TRIP effect (Transformation Induced Plasticity), which significantly influences the cyclic material properties. In this study, a concept is being developed to quantify the fatigue life of this metastable austenite, explicitly considering the load-induced phase transformation. By using the crystal plasticity finite element method (CPFEM) in combination with various three-dimensional, statistically representative volume elements (3D-SRVEs) of the underlying microstructure, the influence of this phase transformation can be investigated numerically on a microscopic scale. When analysing a fatigue indicator parameter (FIP) which is based on the accumulated plastic slip, it can be shown that the TRIP effect has a positive influence on the fatigue life.

INTRODUCTION

Due to their good corrosion resistance metastable, austenitic stainless steels are used in particular in nuclear facilities as piping in the primary and secondary cooling circuit. Cyclic loads often occur during operation, causing the austenitic phase to transform into martensite under load. Due to the different mechanical properties of these two phases, the mechanical behaviour of the respective component also changes considerably. Various authors have already been able to experimentally demonstrate the occurrence of this load-induced phase transformation in the past, e.g. Krupp et al. (2001) or Smaga et al. (2017). However, the focus here was on the macroscopic material behaviour. As this is significantly influenced by the underlying microstructure, it is also important to investigate this phenomenon locally. Since conducting such experiments is very time-consuming and costly, appropriate numerical methods are required. At the same time, these approaches should also be used to predict the component performance so that the evaluation of component safety can subsequently be carried out. With the help of microstructure-sensitive fatigue modelling approaches as proposed by McDowell (2007), these additional requirements can be met. By combining micromechanical material models in the context of CPFEM with 3D-SRVEs, critical variables can be resolved locally. Using appropriate homogenization methods, the material behaviour can then be mapped to a macroscopic scale.

In the literature, various authors have already successfully applied approaches of microstructure-sensitive fatigue modelling to different materials, e.g. Musinski and McDowell (2012), Yaghoobi et al. (2021) or Natkowski et al. (2022). What all these studies have in common, however, is that materials were investigated that do not exhibit a load-induced phase transformation under external loads. Various micromechanical material models for predicting these load-induced phase transformation already exist in the literature. For example, Wong et al. (2016) developed a dislocation-based crystal plasticity model for high manganese steels that can depict the TRIP effect and TWIP (Twinning Induced Plasticity)

effect as an additional deformation mechanism based on the material's stacking fault energy over a wide range of different temperatures.

While this model was developed for the DAMASK framework by Roters et al. (2019), Ma and Hartmaier (2015) proposed a phenomenological model that can predict the TRIP effect for TRIP-assisted steels under quasi-static load for the FEM solver ABAQUS. The latter has even been further developed by Gupta et al. (2018) by considering strain gradients through geometrically necessary dislocations (GNDs), making it a gradient enhanced or non-local crystal plasticity model. Although such models already exist, none have been used to predict cyclic material properties of steels. This is where this study comes in, in which the phenomenological TRIP model developed by Ma and Hartmaier (2015) was used for the first time in the context of microstructure-sensitive fatigue modelling.

GEOMETRIC REPRSENTATION OF THE MICROSTRUCTURE AS 3D-SRVEs

The material examined in this study is an austenitic stainless steel of type AISI 347, which is almost fully austenitic in its initial state, as can be seen from EBSD images in Figure 1. Due to the dimensions of 925 µm x 580 µm, 20,225 grains could be analysed. The determined phase fractions are approximately 99.1% austenite and 0.9% martensite. As this steel grade reacts very sensitively to external loads, it can be assumed that the existing martensite was created during metallographic preparation by mechanical grinding and polishing and could not be completely removed by subsequent electrolytic polishing. For this reason, the martensite was neglected in the generation of the 3D-SRVE, so that only fully austenitic 3D-SRVEs were generated.

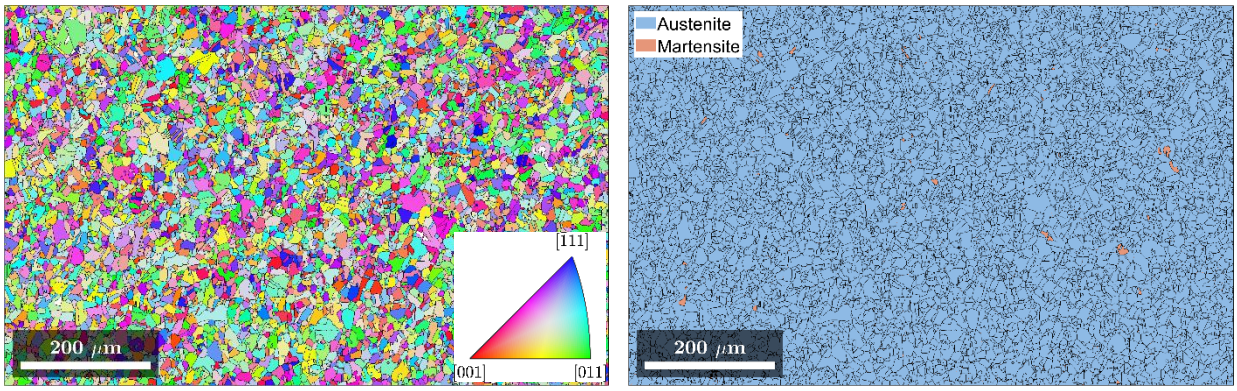

a) Inverse pole figure b) Phase map

Figure 1. EBSD image of AISI 347.

Using the MATLAB toolbox MTEX by Bachmann et al. (2011), statistics regarding grain size, grain morphology and crystallographic orientations were evaluated for the austenite grains. The data collected in this way was then fed into a Wasserstein Generative Adversarial Neural Network (WGAN) proposed by Fehlemann et al. (2021), which, after appropriate training, can generate an infinite number of artificial data sets that correspond to the distribution functions and associated interdependencies of the real underlying microstructure. Figure 2 shows the comparison of the real (orange) and artificial (blue) data after training of 300,000 iterations. Here phi1, PHI and phi2 correspond to the three Euler angles. It can be seen that the synthetic data sets match the real data very well.

The trained, artificial data set can then be fed into the RVE generator called DRAGen (Discrete RVE Automation and Generation) developed by Henrich et al. (2023). This is a generator for two-dimensional or three-dimensional SRVEs, which generates microstructure models from the synthetic input data. These can then be used to carry out numerical simulations within the corresponding simulation framework such as ABAQUS or DAMASK.

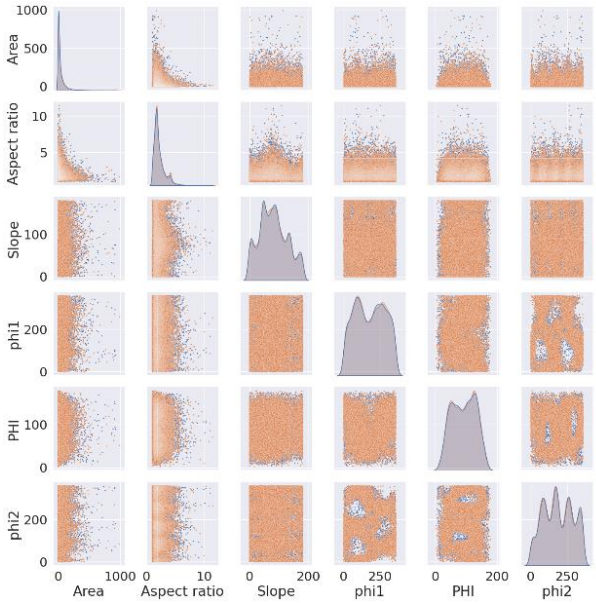

Figure 2. Comparison of real (orange) and artificial (blue) data after training the WGAN.

Since the WGAN can be used to generate an infinite number of artificial data sets, DRAGen can in principle also be used to generate an infinite number of SRVEs. Each SRVE generated in this way is different in that it has a different number of grains, for example, but it still follows the same underlying distribution function of the real data. Due to these differences, the simulation results also deviate within a certain range. For this reason, a total of 10 SRVEs with a boxsize of 50 µm x 50 µm x 50 µm were generated in this study, which contain on average 179±17 grains. Figure 3 shows two of the ten SRVE generated by DRAGen for ABAQUS. These are the two extreme cases with the maximum and minimum number of grains, respectively 201 and 147 grains. The models contain three-dimensional, quadratic elements with reduced integration (C3D8R).

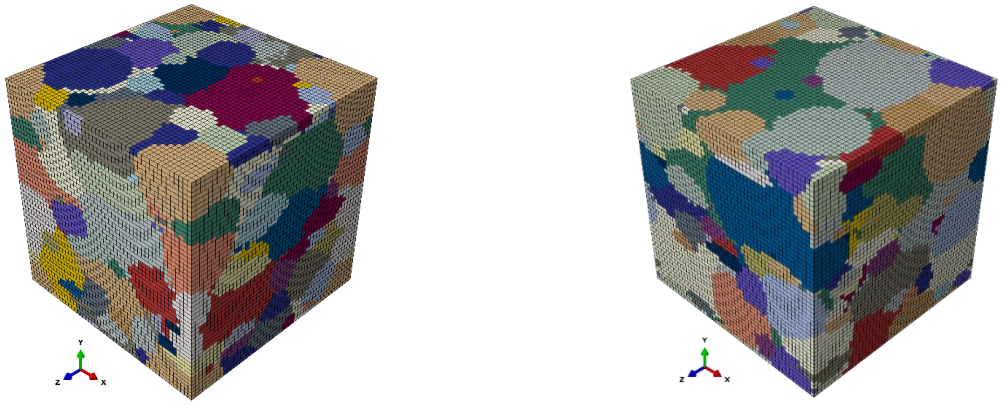

a) SRVE with 201 grains b) SRVE with 147 grains

Figure 3. Exemplary SRVEs generated with DRAGen.

MATERIAL MODEL

Crystal Plasticity Model Considering TRIP

Once the SRVE has been created, a crystal plasticity model is required to carry out simulations. In this study, the phenomenological model of Ma and Hartmaier (2015) was used in the form of a UMAT subroutine for ABAQUS, which explicitly takes into account the load-induced phase transformation of austenite to martensite. Detailed information can be found in Ma and Hartmaier (2015) therefore only the most relevant equations are presented below.

The basic idea is that the deformation gradient $\boldsymbol{F}$ is divided into an elastic part $\boldsymbol{F}_e$ and a plastic part $\boldsymbol{F}_p$. In addition, the TRIP effect is taken into account as an additional deformation mechanism $\boldsymbol{F}_{tr}$ as shown in Equation 1:

$$\boldsymbol{F} = \boldsymbol{F}_e \boldsymbol{F}_p \boldsymbol{F}_{tr} \tag{1}$$

Within the large deformation framework of this model the evolution of the plastic deformation gradient $\boldsymbol{L}_p$ is depending on the shear rate $\dot{\gamma}^{\alpha}$ and the Schmid tensor $\widetilde{\mathbf{M}}^{\boldsymbol{\alpha}}$ of the slip system α (Equation 2):

$$\boldsymbol{L}_p = \dot{\boldsymbol{F}}_p \boldsymbol{F}_p^{-1} = \sum_{\alpha=1}^{12} \dot{\gamma}^{\alpha} \, \widetilde{\mathbf{M}}^{\boldsymbol{\alpha}} \tag{2}$$

The martensite content is divided up additively in this model by differentiating between pre-existing nuclei of martensite η^0, strain induced nucleation η^{strain} and stress assisted growth of martensite η^{stress} which is shown by Equation 3:

$$\eta = \eta^0 + \eta^{strain} + \eta^{stress} \tag{3}$$

Analogous to the evolution of the plastic deformation gradient, the evolution of the deformation gradient for the TRIP effect $\boldsymbol{L}_{tr}$ can be calculated using Equation 4:

$$\boldsymbol{L}_{tr} = \dot{\boldsymbol{F}}_{tr} \boldsymbol{F}_{tr}^{-1} = \sum_{I=1}^{N^T} \dot{\eta}_I^{stress} \, \widetilde{\boldsymbol{N}}_{\boldsymbol{I}} \tag{4}$$

Where $\dot{\eta}_I^{stress}$ is the evolution of the stress assisted martensite growth and $\widetilde{\widetilde{\boldsymbol{N}}_I}$ is the eigen-deformation tensor of the transformation system I. N^T is the total number of transformation systems which is 12 according to the inverse Nishiyama-Wasserman relationship.

The calculation of the resolved shear stress τ^{α} of slip system α can be seen in Equation 5. It depends on the slip direction $\widetilde{\boldsymbol{m}}^{\alpha}$ and normal direction $\widetilde{\boldsymbol{n}}^{\alpha}$of slip system α, as well as the second Piola-Kirchoff stress $\tilde{\boldsymbol{S}}$.

$$\tau^{\alpha} = \tilde{\boldsymbol{S}} \cdot (\widetilde{\boldsymbol{m}}^{\alpha} \otimes \widetilde{\boldsymbol{n}}^{\alpha}) \tag{5}$$

The evolution of the shear rate $\dot{\gamma}^{\alpha}$ on slip system α is expressed by Equation 6:

$$\dot{\gamma}^{\alpha} = \dot{\gamma}_0 \left| \frac{\tau^{\alpha}}{\hat{\tau}_c^{\alpha} + \hat{\tau}_{TRIP}^{\alpha}} \right|^n sgn(\tau^{\alpha}) \tag{6}$$

Where $\dot{\gamma}_0$ and n are material parameters, which represent the reference shear rate and the inverse of the strain rate sensitivity, respectively. $\hat{\tau}_c^{\alpha}$ is the critical resolved shear stress and $\hat{\tau}_{TRIP}^{\alpha}$ is the respective shear rate based on the TRIP effect.

The lamellar hardening of the martensite can be read as follows (see Equation 7), taking into account a fitting parameter c_{mhd} and the shear modulus μ of the martensite phase, as well as the evolution of the total martensite fraction $\dot{\eta}_I$ of transformation system I:

$$\dot{\hat{\tau}}_{TRIP}^{\alpha} = c_{mhd}\mu \sum_{I=1}^{N^T} \dot{\eta}_I \tag{7}$$

Fatigue Indicator Parameter

In order to be able to determine the fatigue properties, a corresponding numerical value is required, which is referred to as fatigue indicator parameter (FIP). In this study, a FIP based on the accumulated plastic slip p_{acc} as presented by Sharaf et al. (2014) is used. The latter is calculated as shown in Equation 8 from the evolution of the plastic deformation gradient (Equation 2), which is also referred to as the plastic velocity gradient:

$$p_{acc} = \int_0^{t'} \sqrt{\frac{2}{3}\boldsymbol{L}_P : \boldsymbol{L}_p}\, dt \tag{8}$$

This accumulated plastic slip was implemented in the model and calculated by the subroutine during the simulation. The actual FIP was then calculated in the post-processing, by calculating the average over the grain volumes and taking the maximum of these values. This results in one single value per simulation frame. See Equation 9:

$$P_{mps} = FIP = max\left(\frac{1}{V^{Gr}} \sum_{i=1}^{N_{el}^{Gr}} p_{acc,i} V_i\right) \tag{9}$$

Here V^{Gr} represents the volume of the observed grain, N_{el}^{Gr} is the number of elements in said grain and $p_{acc,i}$ as well as V_i are the accumulated plastic slip and volume of the *i*-th element within this grain, respectively. This FIP represents persistent slip bands that form through the accumulation of dislocations under cyclic loading, which in turn act as sites for fatigue crack initiation. The validity of this assumption was confirmed simulatively and experimentally by Sharaf et al. (2014).

NUMERICAL RESULTS

A total of 10 different, yet statistically equivalent SRVEs were used for the numerical analysis in this study. In order to be able to depict the macroscopic material behaviour in the simulations, periodic boundary conditions were applied to all SRVEs by DRAGen. The same boundary conditions were used in all simulations by applying a strain amplitude ε_a = 1% in the y-direction at a strain ratio of R = -1. The mean strain was therefore ε_m = 0%, which means that the magnitude of the tensile and compressive load is identical. A total of N = 50 cycles were simulated using a triangular shape with a frequency of f = 0.1 Hz. This allowed a constant strain rate to be realized over the number of cycles applied.

Figure 4 a) shows an example of the simulated evolution of the martensite content for the SRVE with 201 grains. It can be seen that the martensite content increases slightly linearly up to about 15 cycles, until an almost exponential growth occurs, which enters a saturation range at about 40 cycles. Thus, the model can capture the sigmoidal shape over the number of cycles as shown experimentally by Krupp et al. (2008). The resulting hardening through the TRIP effect also has an influence on the true stress in Figure 4 b). The upper and lower peak stresses for a simulation of the same SRVE with and without the TRIP effect are plotted here. It can be observed that a sudden hardening with subsequent saturation also sets in after approx. 15 cycles, just as the martensite content shows. The model is therefore capable of capturing the TRIP effect even under cyclical loads.

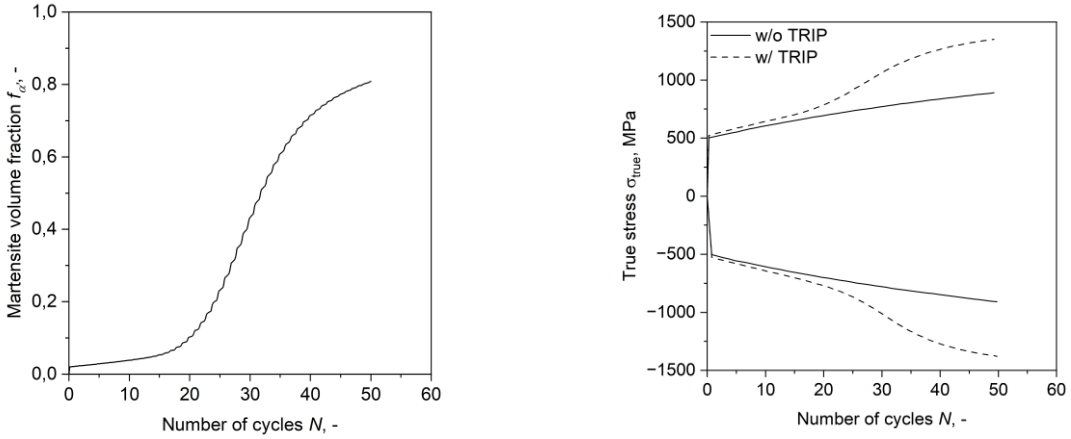

a) Martensite volume fraction b) True stress with and without TRIP

Figure 4. Simulation results of the SRVE with 201 grains.

The change in microstructure composition is shown in Figure 5 on the SRVE. Taking into account the fact that the SRVE was completely austenitic at the beginning, the SRVE also shows this phase transformation after the 25th and 50th cycle, respectively. It can be seen that, depending on the crystallographic orientation, some grains transform earlier than others or in some cases do not transform at all.

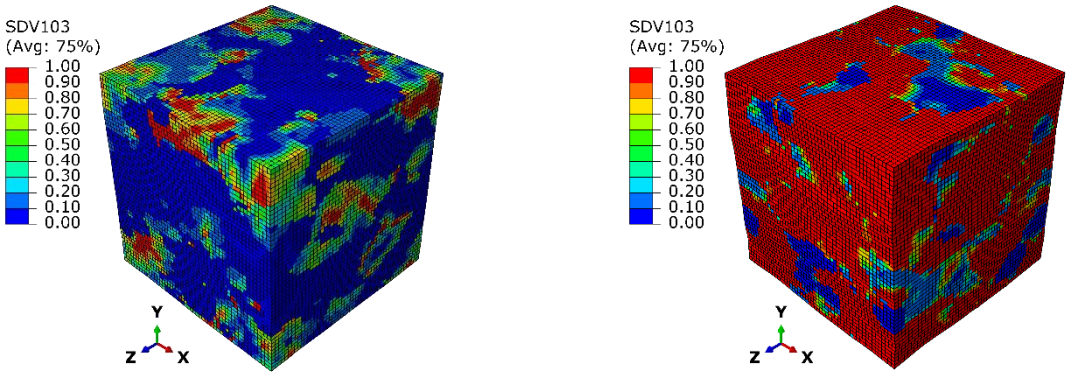

a) 25th cycle b) 50th cycle

Figure 5. Evolution of the martensite volume fraction of the SRVE with 201 grains.

Figure 6 a) shows that the results differ per SRVE using the example of the martensite volume fraction. For this reason, it is necessary to simulate several SRVEs in order to be able to calculate a corresponding mean value from all simulations, which can then be used for further analyses. The mean value across all 10

SRVEs with and without TRIP effect is compared for the FIP used in this study in Figure 6 b). It can be seen that with increasing martensite content, the FIP deviates from the curve without TRIP effect. If a critical value of 2, for example, is assumed here and the number of cycles achieved is read from the graph, it can be seen that the TRIP effect has a positive effect on the fatigue life under cyclic loading, as the critical value is reached at a later point in time.

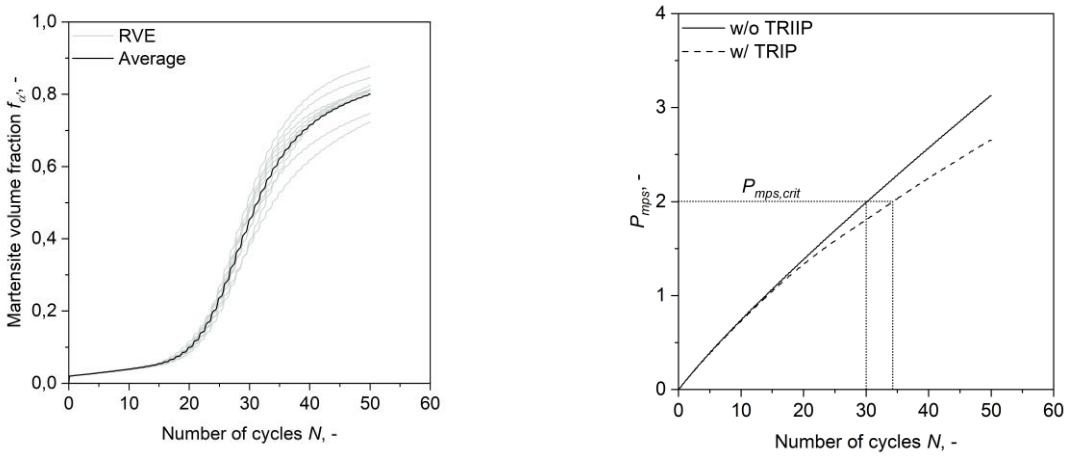

a) Martensite volume fraction b) Fatigue indicator parameter

Figure 6. Averaged simulations results of all 10 SRVE.

CONCLUSION AND OUTLOOK

In this study, a phenomenological crystal plasticity model with consideration of the load-induced phase transformation from austenite to martensite was applied for the first time in the context of microstructure-sensitive fatigue modelling. It could be shown that the evolution of the martensite volume fraction under cyclic load could be modelled and correctly depicts the sigmoidal shape which is reported in literature. Furthermore, it could be shown that the TRIP effect has positive influence on the fatigue life. After calibration of the model parameters to real experimental data, the model can be used to quantitatively estimate the fatigue life for metastable austenitic stainless steels as used in nuclear power plants. In addition, deeper insights into the microscopic material behaviour and transformation behaviour and their effect on the fatigue life can be generated.

ACKNOWLEDGMENTS

Computations were performed with computing resources granted by RWTH Aachen University under project rwth1684. The project is funded by the German Federal Ministry for Environment, Nature Conservation, Nuclear Safety and Consumer Protection (BMUV, project no. 1501656) on basis of a decision by the German Bundestag.

REFERENCES

Bachmann, F., Hiechler, R., Schaeben, H. (2011). "Grain detection from 2d and 3d EBSD data – Specification of the MTEX algorithm", *Ultramicroscopy*, Elsevier B.V., 111, 1720-1733

Fehlemann, N., Sparrer Y., Pütz, F., Könemann, M., Münstermann, S. (2021). "Influence of synthetically generated inclusions on the stress accumulation and concentration in X65 pipeline steel“, *IOP Conf.Ser.: Mater. Sci. Eng.*, 1157, 01205

Gupta, S., Ma, A., Hartmaier, A. (2018). "Mechanical twinning induced alteration in the kinetics of martensitic phase transformation in TRIP-maraging steels", *International Journal of Solids and Structures*, Elsevier Ltd., 155, 213-224

Henrich, M., Fehlemann, N., Bexter, F., Neite, M., Kong, L., Shen, F., Könemann, M., Dölz, M., Münstermann, S. (2023). "DRAGen – A deep learning supported RVE generator framework for complex microstructure models", *Heliyon*, Elsevier Ltd., 9(8), e19003

Krupp U., Christ, H.J., Lezuo, P., Maier, H.J., Teteruk, R.G. (2001). "Influence of carbon concentration on martensitic transformation in metastable austenitic steels under cyclic loading conditions", *Materials Science and Engineering A*, Elsevier B.V., 319, 527-530

Krupp, U., West, C., Christ, H.-J. (2008), "Deformation-induced martensite formation during cyclic deformation of metastable austenitic steel: Influence of temperature and carbon content", *Materials Science and Engineering A*, Elsevier B.V., 481-482, 713-171

Ma, A., Hartmaier, A., (2015). "A study of deformation and phase transformation coupling for TRIP assisted steels", *International Journal of Plasticity*, Elsevier Ltd., 64, 40-55

McDowell, D.L., (2007). "Simulation-based strategies for microstructure-sensitive fatigue modeling", *Materials Science and Engineering A*, Elsevier B.V., 468-470, 4-14

Musinski, W.D., McDowell, D.L., (2012). "Microstructure-sensitive probabilistic modeling of HCF crack initiation and early crack growth in Ni-base superalloy IN100 notched components", *International Journal of Fatigue*, Elsevier Ltd., 37, 41-53

Natkowski, E., Sonnweber-Ribic, P., Münstermann, S., (2022). "Determination of fatigue lifetimes with a micromechanical short crack model for the high-strength steel SAE 4150", *International Journal of Fatigue*, Elsevier Ltd., 156, 106621

Roters, F., Diehl, M., Shanthraj, P., Eisenlohr, P., Reuber, C., Wong, S.L., Maiti, T., Ebrahimi, A., Hochrainer, T., Farbritius, H.O., Nikolov, S., Friák, M., Fujita, N., Grilli, N., Janssens, K.G.F., Jia, N., Kok, P.J.J., Ma, D., Meier, F., Werner, E., Stricker, M., Weygand, D., Raabe, D. (2019), "DAMASK – The Düsseldorf Advanced Material Simulation Kit for modeling multi-physics crystal plasticity, thermal, and damage phenomena from the single crystal up to the component scale", *Computational Materials Science*, Elsevier B.V., 158, 420–478

Sharaf, M., Kucharczyk, P., Vajragupta, N., Münstermann, S., Hartmaier, A., Bleck, W. (2014). "Modeling the microstructure influence on fatigue life variability in structuarl steels", *Computational Materials Science*, Elsevier B.V., 94, 258–272

Smaga, M., Skorupski, R., Eifler, D., Beck, T. (2017). "Microstructural characterization of cyclic deformation behavior of metastable austenitic stainless steel AISI 347 with different surface morphology", *Journal of Materials Research*, SpringerLink, 32, 4452-4460

Wong, S.L., Madivala, M., Prahl, U., Roters, F., Raabe, D. (2016). "A crystal plasticity model for twinning- and transformation-induced plasticity", *Acta Materialia*, Elsevier Ltd., 118, 140-151